CHAPTER VIII

FISCHER-TROPSCH SYNTHESIS: TPR AND XANES ANALYSIS OF THE IMPACT OF SIMULATED REGENERATION CYCLES ON THE REDUCIBILITY OF Co/ALUMINA CATALYSTS WITH DIFFERENT PROMOTERS (Pt, Ru, Re, Ag, Au, Rh, Ir)

8.1 Abstract

The goal of this work is to explore the ability of the metal-promoted 25%Co/Al_2O_3 catalyst to maintain good contact between the metal and cobalt and continue facilitating Co oxide reduction after simulated regeneration cycles through oxidation-reduction treatments, an approach designed to simulate the catalyst regeneration process. Unpromoted 25%Co/Al_2O_3 catalyst was also subjected to treatements and served as a reference. Seven metal promoters were examined in this work, including Pt. Ru, Re, Ag, Au, Rh, and Ir. Fresh and treated catalysts were evaluated by both TPR and XANES spectroscopy, the latter approach utilizing linear combination fittings with appropriate reference compounds. With the unpromoted catalyst, oxidation-reduction cycles tended to have two effects: (1) a fraction of CoO species that lost their interaction with the support emerged and (2) a fraction of more strongly interacting CoO species was formed. A comparison between the freshly calcined sample and samples subjected to simulated regeneration cycles was demonstrated. Pt-, Ru-, Re-, Ag-, and Rh-promoted 25%Co/Al_2O_3 catalysts maintained their ability to facilitate Co oxide reduction after undergoing oxidation-reduction cycles even up to 3 cycles, while with Ir- and, especially, Au-25%Co/Al_2O_3 some losses were observed, suggesting some separation between the promoter and cobalt occurred following the treatment cycles. TPR profiles also suggest that some separation of Ru from Co occurs with simulated regeneration cycles, although it does not impact the extent of reduction of Co after three cycles.

Keywords: Regeneration, Oxidation-reduction cycles, Co/Al_2O_3 catalyst, Platinum (Pt), Ruthenium (Ru), Rhenium (Re), Silver (Ag), Gold (Au), Rhodium (Rh), Iridium (Ir)

8.2 Introduction

Co/alumina is well-known as a Fischer-Tropsch synthesis catalyst for gas-to-liquids (GTL) processes, and the cobalt metal surface sites likely serve as active sites for the reaction. The interaction between cobalt and alumina support is very strong (Espinoza et al., 1998; Van Berge et al., 2001), thereby making cobalt oxides difficult to reduce. This feature is also, however, important for the stabilization of small cobalt clusters for reaction (Jacobs et al., 2002). If the clusters are too small (e.g., having crystallites < 2 nm (van Steen et al., 2005)), however, they are susceptible to oxidation at high conversions due to the high partial pressure of H_2O relative to reducing gases present (Jacobs et al., 2004; Jongsomjit et al., 2001; Ma et al., 2011; Schanke et al., 1995; van Berge et al., 2000). Therefore, to stabilize the clusters against deactivation by oxidation, high Co loadings (20+ % by wt.) are typically used (Van Berge et al., 2001) and the addition of metal promoter is employed to facilitate the reduction of cobalt oxide species. This may be via a H_2 dissociation and spillover mechanism or chemical promotion (Jacobs et al., 2004; Jacobs et al., 2002; Jacobs et al., 2007).

Noble metals are primarily used to facilitate the reduction of cobalt oxides and thereby increase surface Co^0 site densities (Jacobs et al., 2002). Moreover, they are reduced to the metallic phase at lower temperatures compared to Co, thus providing metal surface sties that presumably chemisorb and dissociate H_2, that in turn allows Co^0 nuclei to germinate. Metal promoters such as Pt, Ru, and Re (Arnoldy et al., 1985; Das et al., 2003; Jacobs et al., 2004; Jacobs et al., 2002; Jacobs et al., 2007; Kogelbauer et al., 1996; Rygh et al., 2000; Schanke et al., 1995) are commonly employed to facilitate the reduction of Co oxides in Co/alumina catalysts. An improvement in reducibility by adding these promoters also translates to an increase in Co metal site densities and, respectively, an increase in activity of the Co/alumina catalyst on a per gram catalyst basis. Note that turnover frequency on a per site basis typically remains unaltered (Das et al., 2003).

However, a study on the effect of Pt loading by our group (Jermwongratanachai et al., 2013) revealed that although adding higher loadings of Pt enhances the reducibility of the catalyst, it detrimentally affects FT product

selectivity (i.e., slightly increase CH_4 and CO_2, at disadvantage to C_5+). Palladium (Pd) as a promoter was also studied by our group (Jacobs et al., 2012). Unlike Pt, Ru, and Re addition, Pd addition deleteriously affects the FT product selectivity even at relatively low loading. A study of Ir promoter was reported in a comparison with Pt and Ru promoter, and the results suggested that the efficiency of Co oxide reduction is Ir > Pt > Ru, both at lower and higher amounts (Bianchi, 2001). Moreover, using Group 11 (Cu, Ag, Au) as metal promoters was also reported (Jacobs et al., 2009). Cu facilitates Co oxide reduction, but the increased fraction of reduced Co did not translate to improved active site densities; moreover, it also results in a decrease in CO conversion and an increase in light product selectivity (Jacobs et al., 2009). Small quantities of gold (Au) are known to increase the reducibility of cobalt oxides (Leite et al., 2002), moreover, improved CO conversion, slight decreases in light product selectivity with slight increases in C_5+ selectivity are obtained (Jacobs et al., 2009). Ag promoter provides not only a significant gain in Co active site densities, but also a remarkably improved CO conversion together with slightly improved FT product selectivity (Jacobs et al., 2009). These results of Ag promotion still hold true even at higher Ag loadings (Jermwongratanachai et al., 2013).

The efficiency of each metal promoter in facilitating Co oxide reduction in Co/alumina catalysts has already been elucidated, as described in the literature reference above. However, the ability of each metal promoted catalyst to maintain good contact between cobalt and metal promoter and to continue facilitating Co oxide reduction after oxidation-reduction cycles (e.g., mimicking a catalyst regeneration process), is less understood. Therefore, the objective of the present work is to investigate this aspect. Unpromoted 25%Co/Al_2O_3 and promoted 25%Co/Al_2O_3 catalysts, including Pt-, Ru-, Re-, Ag-, Au-, Rh-, and Ir-promoted catalysts, underwent a series of oxidation-reduction cycles. Between each cycle, a fraction of catalyst was withdrawn to evaluate the reducibility using TPR. Moreover, the oxidation state of Co (after activation in H_2) after each initial activation, and following re-reduction with each oxidation cycle, was determined using XANES spectroscopy.

8.3 Experimental

8.3.1 Catalyst Preparation and Sample Preparation

A slurry impregnation method following a Sasol patent (Espinoza et al., 1998) was used to prepare a parent batch (120 g) of 25%Co/Al_2O_3 catalyst. Sasol Catalox-150 γ-Al_2O_3 was used as a catalyst support, while cobalt nitrate hexahydrate ($Co(NO_3)2•6H_2O$) served as the Co precursor in the loading solution. To achieve 25%Co loading, a 2-step slurry impregnation was applied, whereby the amount of loading solution in each impregnation step was 2.5 times that of the pore volume. Between each impregnation step, the catalyst was dried under vacuum in a rotary evaporator. After finishing the last step of Co addition, the parent batch of 25%Co/Al_2O_3 catalyst was not calcined, but instead split into several small batches in order to prepare smaller batches of metal promoted 25%Co/Al_2O_3 catalysts, while some of 25%Co/Al_2O_3 was kept as a reference. Seven different metals were added separately to each smaller batch, including platinum (Pt), ruthenium (Ru), rhenium (Re), silver (Ag), gold (Au), rhodium (Rh), and iridium (Ir). These metals served as reduction promoters to facilitate reduction of cobalt oxides during catalyst activation. All of promoter metals were added to the catalyst by incipient wetness impregnation (IWI) with metal loading atomically equivalent to 1.0% by wt. Pt. The metal precursors of the promoters used in this work were tetra-amine platinum (II) nitrate, ruthenium nitrosyl nitrate, rhenium (VII) oxide, silver (I) nitrate, gold (III) chloride trihydrate, rhodium (III) chloride hydrate, and iridium (III) chloride hydrate. After adding metal promoter, the catalysts were again dried in the rotary evaporator. Finally, the catalysts were calcined under air flow at 350 °C for 4 h. To ensure removal of Cl^- ions from the Au, Rh, and Ir-promoted catalysts, the calcined catalysts were washed with 1 molar aqueous NH_4OH, dried, and recalcined at 200 °C for 2 h.

As a preliminary evaluation of the potential for each catalyst to be regenerated, oxidation-reduction cycles were performed for both unpromoted 25%Co/Al_2O_3 and all metal promoted 25%Co/Al_2O_3 catalysts. First, the freshly calcined catalysts were reduced at 350 °C for 10 h under flowing 25% H_2/He, cooled to room temperature under H_2 flow and purged with nitrogen and, subsequently passivated by 1% O_2 in nitrogen flow at room temperature. Then, oxidation was

performed at 350 °C for 4 h under flow of air. Three cycles of oxidation-reduction were implemented for each catalyst. The catalyst samples were withdrawn after each cycle for the purpose of characterization by TPR and XANES at the Co K-edge. The question we were interested in answering in this preliminary evaluation was whether or not the promoter can continue to function to facilitate the reduction of cobalt oxides following simulated regeneration of the catalyst via oxidation-reduction cycles. In this work, the following nomenclature is applied. Note that the original calcined catalyst is referred to as "fresh", while reduction of it yields the "freshly activated" catalyst. If the calcined catalyst underwent one reduction-oxidation cycle to simulate regeneration, it is defined as "RO1". If the same catalyst is then reduced and is being examined in its reduced state, it is labeled "activated RO1". If the same "activated RO1" catalyst is subjected to a second oxidation cycle, but remains in the oxidized state, it is referred to as "RO2", and so on.

To prepare reduced samples for XANES experiments after initial activation or following oxidation-reduction cycles, each catalyst was pressed into a flat pellet inside a 1" I.D. reactor with boron nitride. A flow of 80 sccm of hydrogen was then started. The reactor was slowly (100 °C/h) brought up to a standard activation temperature of 350°C and held for 10 h. A separate steel tube was filled with Polywax 725 at 1 atm and heated to 200 °C under N_2 flow (20 sccm). The reactor was cooled to 220 °C and held at this temperature. Next, the reactor was closed and H2 flow was stopped, flow to the reactor containing the polywax was reversed and the polywax was pushed into the reactor containing the cobalt catalyst to encapsulate the pellet in polywax and prevent oxidation from occurring.

8.3.2 Temperature Programmed Reduction (TPR)

Temperature programmed reduction (TPR) profiles of calcined catalysts were recorded using a Zeton-Altamira AMI-200 unit equipped with a thermal conductivity detector (TCD). Samples were pretreated by purging with argon flow at 350 °C to remove traces of water. The TPR was performed using a 10%H_2/Ar gas mixture (referenced to argon) at a flow rate of 30 cm^3/min. The catalyst samples were heated from 50 to 900°C.

8.3.3 X-ray Absorption Near Edge Structure Spectroscopy (XANES)

XANES measurements on catalysts as well as references were conducted at the National Synchrotron Light Source (NSLS) at Brookhaven National Laboratory (beamline X-18b), Upton, New York. The beamline at NSLS was equipped with a Si(111) channel-cut monochromator. A crystal detuning procedure was employed to prevent glitches arising from harmonics. The second crystal of the channel-cut monochromator is weakly linked to the crystal and slightly spring loaded. The other side is a picomotor, a very fine high-pitch screw that turns by piezo, which allows for slight detuning of the crystal. The X-ray ring at the NSLS has a flux of 1×10^{10} photons s^{-1} at 100 mA and 2.5 GeV, and the energy-range capability at X18b is 5.8-40 keV. All catalyst samples were prepared at CAER in the form of catalyst particles embedded in polywax (i.e., with storage in inert gas) as previously described. XANES/EXAFS spectra were recorded at the cobalt K-edge (7.709 keV) in transmission mode and a Co metallic foil spectrum was measured simultaneously with each sample spectrum for the purpose of energy calibration.

XANES spectra were processed using the WinXAS program. A simultaneous pre- and post-edge background removal step was carried out using 2 polynomials (degree 2) and the resulting spectra were normalized by dividing by the height of the absorption edge. Normalized XANES spectra were compared with those of references (Co foil and CoO). Note that CoO spectrum obtained from the TPR-XANES spectrum of 0.5%Pt-25%Co/Al_2O_3 catalyst as it is a more pertinent reference spectrum for CoO from the catalyst. A linear combination fitting was also conducted to quantify the percentage of Co metal presenting in catalyst after reduction using those two Co compounds as references for the fitting.

8.3.4 X-ray Diffraction (XRD)

Powder diffractograms on calcined catalysts were recorded using a Philips X'Pert diffractometer. The long time scan was used over a short range in order to quantify average Co_3O_4 domain sizes using line broadening analysis for the peak at $2\theta = 37°$ representing (311). The conditions are a scan rate of 0.01 °/step and a scan time of 30 s/step over a 2θ range of 30-45°.

8.3.5 Inductively Coupled Plasma Optical Emission Spectrometry (ICP-OES)

Freshly calcined sample and RO3 treated sample (underwent 3 cycles of oxidation-reduction) of each metal promoted catalyst were brought to perform elemental analysis in order to check if metal promoter volatiles during the cycles. The weighed samples were digested using an aqua regia solution, a mixture of concentrated nitric and hydrochloric acids optimally in a volume ratio of 1 : 3 and, then, diluted using a volumetric flask. The sample solutions were aspirated into a Varian 720-ES ICP optical emission spectrometer.

8.4 Results and Discussion

8.4.1 Crystal Size and Elemental Analysis

XRD line broadening analyses of the freshly calcined unpromoted and promoted catalysts revealed that the Co^0 cluster size, assuming a 0.75 contraction from the calculated Co_3O_4 diameter following reduction, was approximately 10 nm in each case. To determine if any significant mass loss was observed after three oxidation-reduction cycles (RO3), ICP was conducted on fresh and RO3 catalysts. No statistically significant difference in promoter concentration was observed as shown in Table 8.1, indicating that the promoter did not volatilize to a significant extent due to the treatments.

8.4.2 Temperature Programmed Reduction

TPR profiles of unpromoted 25%Co/Al_2O_3 are shown in Figure 8.1, and consist of the freshly calcined catalyst, and the catalyst after performing 1, 2, or 3 cycles whereby the catalyst was subjected to successive reduction and oxidation treatments. It is widely accepted that the first peak represents the first step of reduction of Co_3O_4: $Co_3O_4 + H_2 \rightarrow 3CoO + H_2O$, while the second peak represents a subsequent reduction reaction of CoO: $3CoO + 3H_2 \rightarrow 3Co^0 + 3H_2O$ (Jacobs et al., 2007). The stoichiometry of three times the H_2 consumption of the second reaction compared to the first reaction is also in agreement with an area ratio of the second peak to the first peak in TPR profiles.

Table 8.1 Elemental analysis results of fresh and RO3 treated samples of metal promoted 25%Co/Al_2O_3 catalysts

Catalyst	Metal content (%wt)	
	fresh	RO3 treated
1.0%Pt-25%Co/Al_2O_3	0.86	0.82
0.52%Ru-25%Co/Al_2O_3	0.48	0.56
0.95%Re-25%Co/Al_2O_3	0.82	0.81
0.55%Ag-25%Co/Al_2O_3	0.59	0.55
1.0%Au-25%Co/Al_2O_3	0.98	0.97
0.53%Rh-25%Co/Al_2O_3	0.46	0.49
0.99%Ir-25%Co/Al_2O_3	1.17	1.09

The first TPR peak of the freshly calcined catalyst is located at 300 °C, while the second peak is situated at 500 °C with a small shoulder at ~640 °C. This small shoulder is likely attributed to a smaller CoO species strongly interacting with Al_2O_3 support (Jacobs et al., 2002). After undergoing cycles involving reduction and oxidation to simulate regeneration, the TPR profile changed, such that the first and second peaks shifted slightly to higher temperature, while the high temperature shoulder peak of the second peak grew in intensity and shifted to higher temperature. Moreover, a high temperature feature formed at the high temperature side of the first low temperature peak. This has been assigned previously to the reduction of larger CoO particles that lose their interaction with the support (Jacobs et al., 2002). The changes in TPR profiles thus suggest that the simulated regeneration cycles lead to a fraction of larger CoO particles resulting from agglomeration, as well as a fraction of CoO species that are in stronger interaction with the alumina support.

The TPR profiles of metal promoted 25%Co/Al_2O_3 catalysts are illustrated in Figure 8.2. The TPR profile of 1.0%Pt-25%Co/Al_2O_3 catalyst in Figure 8.2(A) shows that, by comparison with unpromoted catalyst, Pt is able to significantly facilitate Co oxide reduction (i.e., -140 °C shift for the first peak and -

120 °C shift for the second peak compared to unpromoted catalyst). This is in agreement with previous reports (Jacobs et al., 2004; Jacobs et al., 2002; Jacobs et al., 2007; Jermwongratanachai et al., 2013; Schanke et al., 1995). After cycles involving reduction and oxidation, Pt maintains its promoting effect, suggesting that Pt still remains in contact with Co oxide to assist in accelerating the reduction of Co oxides, perhaps by a H_2 dissociation and spillover mechanism (Jacobs et al., 2004; Jacobs et al., 2002; Jacobs et al., 2007).

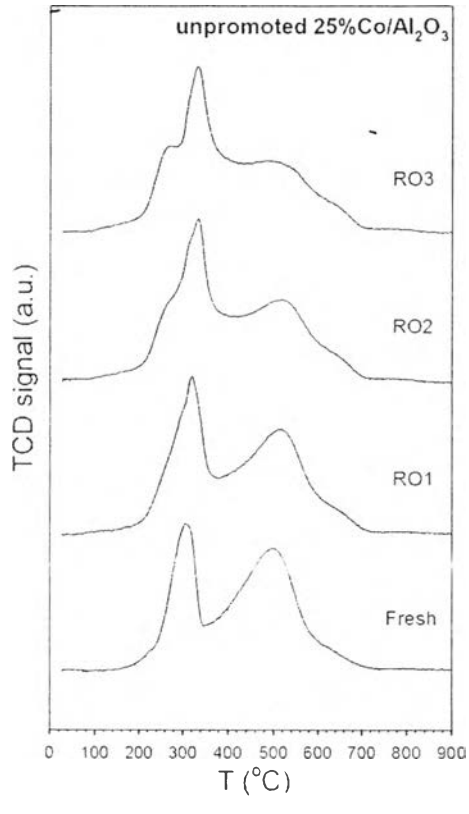

Figure 8.1 Comparative TPR spectra of unpromoted 25%Co/Al_2O_3 catalysts before and after simulated regeneration cycles including after 1 cycle (RO1), 2 cycles (RO2), and 3 cycles (RO3).

Moreover, the first peak and, especially, the second peak shift to lower temperatures with cycling treatments. They appear at ~145 °C and ~320 °C, respectively, and remained at almost precisely the same temperature even after undergoing three

simulated regeneration cycles. Therefore, the preliminary findings indicate that enough Pt is in close enough proximity to continue its function in facilitating cobalt oxide reduction. For 0.52%Ru-25%Co/Al_2O_3 catalyst, the TPR profile in Figure 8.2(B) confirms a role of Ru as a metal promoter, in which the reduction temperature of the first and the second peak shift to lower compared to unpromoted catalyst. After cycles involving reduction and oxidation, the shapes of TPR profiles are obviously changed, suggesting structural changes in coordination between the promoter and cobalt. Unlike Pt-promoted catalyst, Ru-promoted catalyst tends to be more difficult to reduce after simulated regeneration cycles as the temperature of the second peak in TPR slightly increases with the number of treatment cycles. However, the temperature of the second peak is still lower than that of the unpromoted catalyst, so that the ability of this catalyst to regenerate is still satisfactory after three cycles. Figure 8.2(C) depicts the TPR profiles of 0.95%Re-25%Co/Al_2O_3 catalyst. The profiles also confirms the role of Re in facilitating Co oxide reduction. This holds true even after three simulated regeneration cycles. In this catalyst, the promotion by Re occurs after the first step of reduction of Co_3O_4 since Re oxide reduces at ~347 °C (Jacobs et al., 2002) while Co_3O_4 reduce at ~310 °C, such that Re metal plays a significant role in facilitating primarily the reduction of CoO; a shift in the second peak to lower temperature is evident. After simulated regeneration cycles, the temperature of the second peak is slightly lower than that of the freshly calcined catalyst and still remains at the same temperature (i.e., ~360 °C) even up to 3 cycles of reduction and oxidation. Like the case of Pt, Re does an excellent job in maintaining its ability to facilitate reduction. In the case of 0.55%Ag-25%Co/Al_2O_3 catalyst, the TPR profile in Figure 8.2(D) shows that Ag exhibits a good ability to facilitate Co oxide reduction. The first peak shifts to ~245 °C (Δ = -65 °C) while the second peak shifts to ~410 °C (Δ = -92 °C). After simulated regeneration cycles, the profile shape is slightly changed but there is a new peak that forms at the high temperature side of the first peak, and this is likely due to a fraction of Co with a larger size that loses some interaction with the support. Nonetheless, the reduction temperature of the second peak still remains almost the same as that of the freshly calcined catalyst. Therefore, Ag continues to facilitate the reduction of cobalt oxides even after simulated regeneration cycles. TPR profiles of

1.0%Au-25%Co/Al_2O_3 catalyst in Figure 8.2(E) illustrate that although Au can facilitate Co oxide reduction, its ability to do so becomes worse after cycles of reduction and oxidation, as the temperatures of reduction of the first and second peaks clearly shift to higher temperatures. Moreover, those temperatures appear to slightly increase with increasing number of simulated regeneration cycles, indicating that Au apparently separates from Co during regeneration, and added complexity for the development of this catalyst. That is, a different regeneration treatment other than air may be required. Figure 8.2(F) represents the TPR profiles of 0.53%Rh-25%Co/Al_2O_3 catalyst. It was observed that Rh plays a significant role in facilitating Co oxide reduction. The first peak shifts to ~180 °C and the second peak shifts to ~360 °C. The ability of Rh to facilitate Co oxide reduction seems to be close to that of Pt. Furthermore, Rh also maintains its ability to facilitate Co oxide reduction after simulated regeneration cycles. Like Pt-promoted catalyst, Rh-promoted catalyst provides similar profiles after reduction and oxidation cycles, such that the temperature of the second peak of the catalyst after successive treatment cycles is lower than that of the freshly calcined catalyst. Figure 8.2(G) shows TPR profiles of 0.99%Ir-25%Co/Al_2O_3 catalyst. It is obvious that Ir is also able to facilitate the reduction of Co oxide. Although after simulated regeneration cycles, the shape of the TPR profiles changed significantly, especially after the 2^{nd} and 3^{rd} cycles, the temperature of the second peak still remained relatively close to that of the freshly calcined catalyst. This suggests that Ir still maintains its ability to facilitate Co oxide reduction after treatment cycles, but that some separation between Co and Ir likely occurred.

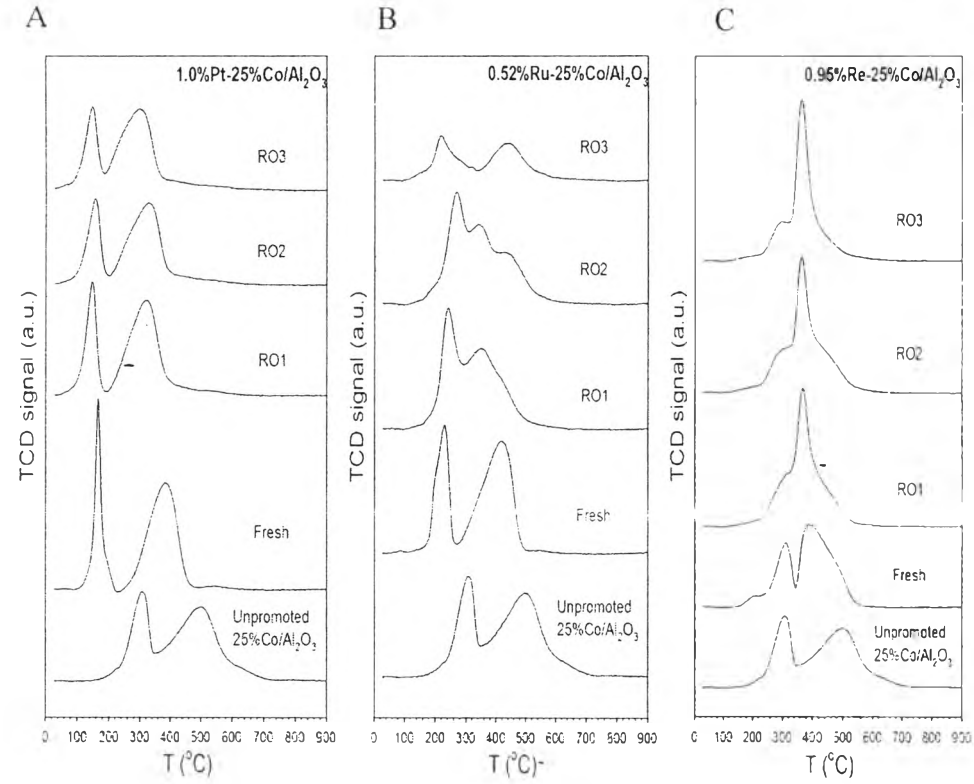
A
B
C
1.0%Pt-25%Co/Al2O3
0.52%Ru-25%Co/Al2O3
0.95%Re-25%Co/Al2O3
RO3
RO2
RO1
Fresh
Unpromoted 25%Co/Al2O3
TCD signal (a.u.)
T (°C)
0 100 200 300 400 500 600 700 800 900

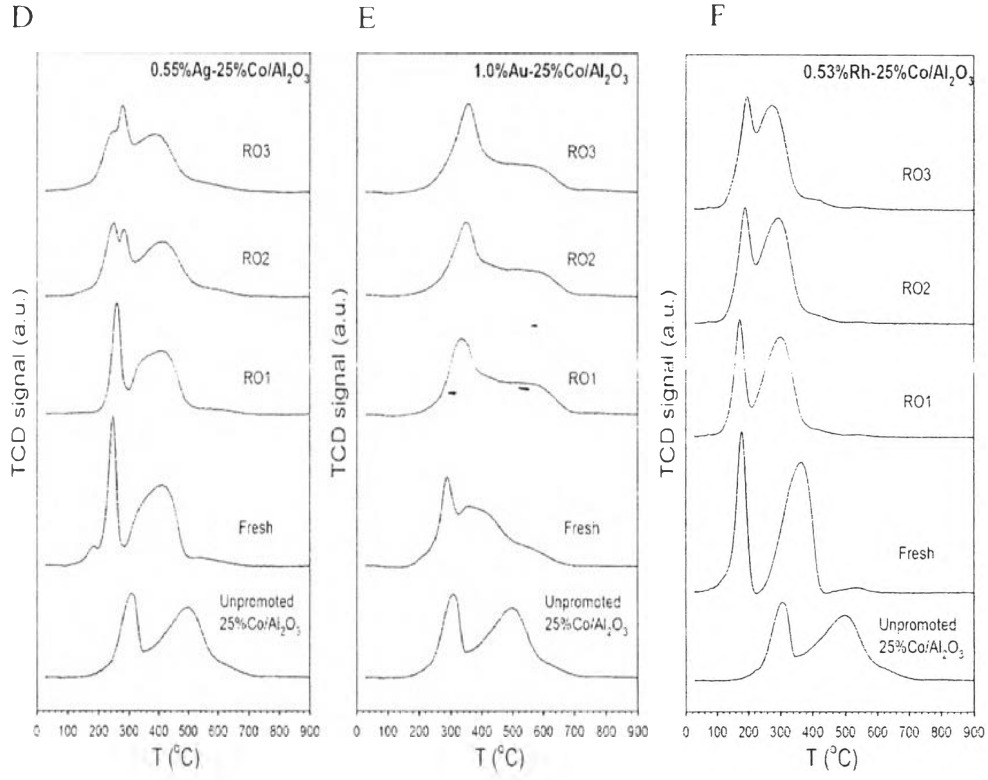
D
E
F
0.55%Ag-25%Co/Al2O3
1.0%Au-25%Co/Al2O3
0.53%Rh-25%Co/Al2O3
RO3
RO2
RO1
Fresh
Unpromoted 25%Co/Al2O3
TCD signal (a.u.)
T (°C)
0 100 200 300 400 500 600 700 800 900

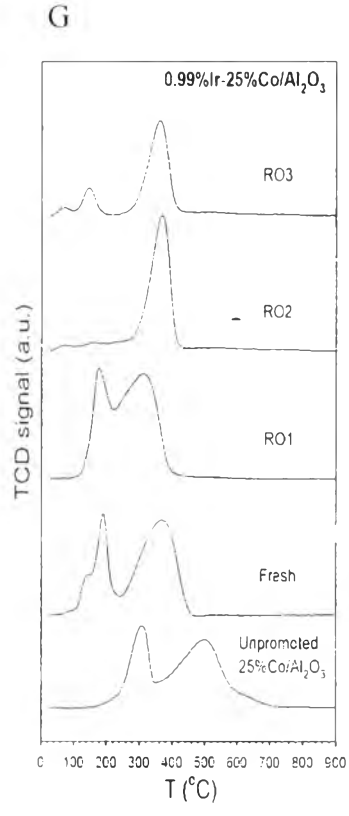

Figure 8.2 Comparative TPR spectra of unpromoted 25%Co/Al_2O_3 catalyst (bottom) with metal promoted 25%Co/Al_2O_3 catalysts before and after simulated regeneration cycles, including (A) 1.0%Pt-25%Co/Al_2O_3, (B) 0.52%Ru-25%Co/Al_2O_3, (C) 0.95%Re-25%Co/Al_2O_3, (D) 0.55%Ag-25%Co/Al_2O_3, (E) 1.0%Au-25%Co/Al_2O_3, (F) 0.53%Rh-25%Co/Al_2O_3 (G) 0.99%Ir-25%Co/Al_2O_3, including after 1 cycle (RO1), 2 cycles (RO2), and 3 cycles (RO3).

8.4.3 XANES and Linear Combination (LC) Fitting

Figure 8.3 shows normalized XANES spectra at the Co K-edge of each catalyst before and after oxidation-reduction cycles compared to two reference Co compounds, which are a Co foil and CoO extracted from a TPR-XANES run over 0.5%Pt-25%Co/Al_2O_3 (Jacobs et al., 2007). Three samples of each catalyst, including freshly calcined, activated RO1 catalyst (catalyst underwent simulated regeneration cycle), and activated RO2 catalyst, were examined for XANES measurements. Prior to scanning the samples, they were pre-reduced at 350 °C for 10 h in flowing H_2.

The extent of Co reduction following each treatment was investigated. Considering normalized XANES spectra of 0.5%Pt-25%Co/Al_2O_3 catalyst in Figure 8.3(A), the XANES spectrum of the freshly reduced catalyst indicates a high extent of reduction. After simulated regeneration cycles, the spectra of treated samples (i.e., activated RO1 and activated RO2) are almost the same in white line intensity as those of the freshly reduced sample. This is good evidence confirming the role of Pt in facilitating Co oxide reduction even after simulated regeneration cycles, and in good agreement with TPR results (Figure 8.2(A)). Quantitative analysis of the XANES results was also performed by linear combination fitting using the XANES spectra of Co metal and CoO as references, and the results are quantified in Table 8.2. After reduction, the Pt-promoted Co/alumina catalyst contains more than 70% of Co metal and this amount is maintained even after simulated regeneration cycles. Previously, Pt-Co coordination was explored in Pt promoted Co/Al_2O_3 catalyst and it is presumably the desired structure that facilitates Co oxide reduction (Cook et al., 2012; Guczi et al., 2002; Jacobs et al., 2004; Sadeqzadeh et al., 2011). The preference of Pt to coordinate with Co was also revealed in our recent report (Jermwongratanachai et al., 2013) demonstrating that, even up to 5.0% by wt. Pt, Pt-Co coordination predominates, indicating that Pt-Co alloy formation is likely. From this point of view, proximity of Pt to Co is likely maintained after simulated regeneration cycles, since there are no significant changes in TPR and XANES results. Normalized XANES spectra of the 0.52%Ru-25%Co/Al_2O_3 catalyst are depicted in Figure 8.3(B). In agreement with the TPR results discussed previously, Ru facilitates the reduction of Co oxide even after simulated regeneration cycles. The normalized XANES spectra further underscore this conclusion by comparing the spectra of fresh and treated samples; moreover, it is obvious from the percentage of Co metal in Table 8.2 that the amount of Co metal is maintained above 75% after simulated regeneration cycles and following activation of the treated catalyst. The promotion of Ru may be described by Ru-Co alloy formation, which was suggested in our previous EXAFS work (Jacobs et al., 2007), as well as that of Iglesia et al. (Iglesia et al., 1993) who used TiO_2 as the support.

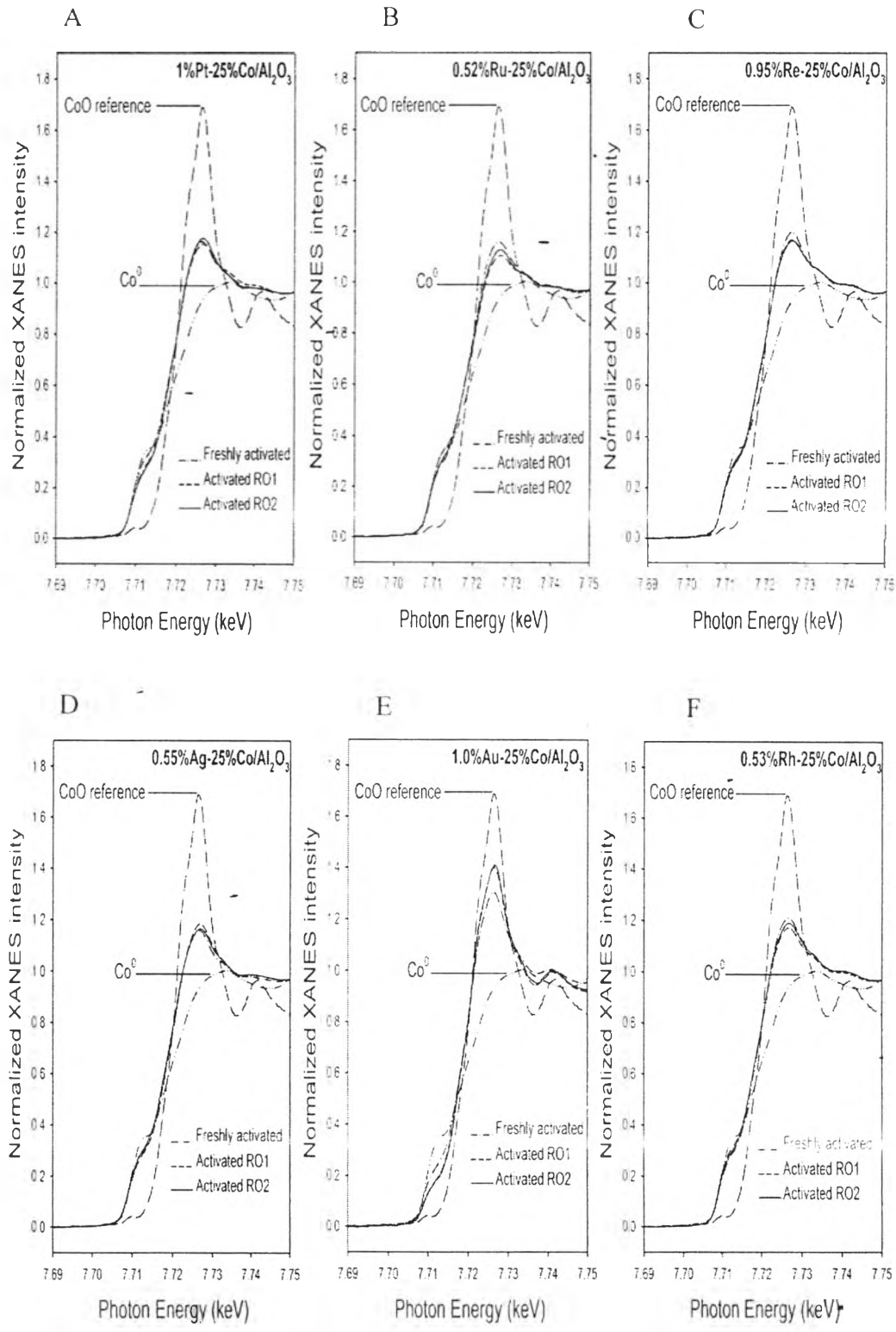
A
B
C
1%Pt-25%Co/Al2O3
0.52%Ru-25%Co/Al2O3
0.95%Re-25%Co/Al2O3
CoO reference
Co0
Freshly activated
Activated RO1
Activated RO2
Normalized XANES intensity
Photon Energy (keV)
D
E
F
0.55%Ag-25%Co/Al2O3
1.0%Au-25%Co/Al2O3
0.53%Rh-25%Co/Al2O3

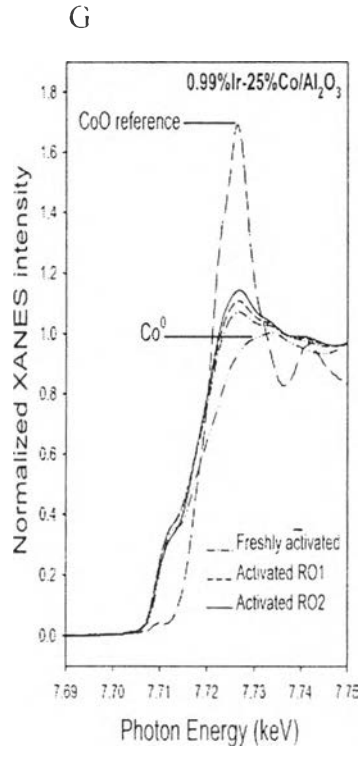

Figure 8.3 Normalized XANES spectra at the Co K-edge of cobalt reference compounds compared to metal promoted 25%Co/Al_2O_3 catalysts before and after simulated regeneration cycles, including (A) 1.0%Pt-25%Co/Al_2O_3, (B) 0.52%Ru-25%Co/Al_2O_3, (C) 0.95%Re-25%Co/Al_2O_3, (D) 0.55%Ag-25%Co/Al_2O_3, (E) 1.0%Au-25%Co/Al_2O_3, (F) 0.53%Rh-25%Co/Al_2O_3, and (G) 0.99%Ir-25%Co/Al_2O_3, including after 1 cycle (Activated RO1) or 2 cycles (Activated RO2).

Notwithstanding, TPR results suggest that some separation between Ru and Co is occurring with oxidation-reduction cycles, such that further cycling could diminish the extent of reduction, though this was not confirmed in this work. The normalized XANES spectra of the 0.95%Re-25%Co/Al_2O_3 catalyst are shown in Figure 8.3(C). It is clear that XANES spectra of treated samples (i.e., activated RO1 and activated RO2) remained close to the XANES spectrum of the freshly reduced catalyst, as virtually the same white line intensity was retained. Moreover, the quantitative results in Table 8.2 also show that more than 70% Co metal is maintained even after simulated regeneration cycles (and re-activation of the catalyst). This is in good agreement with the TPR result in Figure 8.2(C). Previous studies on Re-promoted

Co catalysts by EXAFS showed the formation of Re-Co coordination and this coordination was believed to be important in facilitating Co oxide reduction (Bazin et al., 2002; Jacobs et al., 2004; Rønning et al., 2001). Therefore, the ability of Re to continue to promote Co oxide reduction after undergoing oxidation-reduction cycles suggests the tendency of Re to remain in contact with Co after simulated regeneration cycles. Figure 8.3(D) portrays the normalized XANES spectra of 0.55%Ag-25%Co/Al_2O_3 catalyst. The result is promising and in good agreement with the TPR profiles in Figure 8.2(D). The XANES spectra of the re-activated RO1 and RO2 catalyst samples still retained high extents of reduction; the white line peak intensities were almost the same as that of the freshly reduced sample. The LC fitting results in Table 8.2 also show that after simulated regeneration cycles this catalyst maintains more than 70% Co metal. Not only is Ag-Co coordination found, but also Ag-Ag coordination is present in this catalyst (Jermwongratanachai et al., 2013). The proximity of Ag to Co, as Ag-Co coordination, was suggested to facilitate reduction of Co oxide. Thus, a fraction of Ag promoter most likely remains in proximity to Co to continue facilitating Co oxide reduction after simulated regeneration cycles. As we continue to explore the possibility that Ag, which is much less expensive relative to alternate promoters, may be used as a substitute, the result provides another benefit of Ag, in addition to its capabilities of facilitating Co oxide reduction and improving FT product selectivity (i.e., slightly increase C_5+ and slightly decrease CH_4 and CO_2) that we reported before (Jacobs et al., 2009). Figure 8.3(E) shows the normalized XANES spectra of 1.0%Au-25%Co/Al_2O_3 catalyst. Unlike previous metals, Au displays a clear problem. By LC fitting of XANES spectra, the fresh catalyst contains Co metal of ~60% wt. After simulated regeneration cycles, it is obvious that the ability of Au to facilitate Co oxide reduction diminishes. XANES spectra of activated RO1 and activated RO2 samples are almost identical to each other, but significantly different from the freshly reduced catalyst sample. The higher white line intensity of treated samples compared to those of the fresh sample suggest that Au is separating from cobalt after simulated regeneration cycles. Table 8.2 shows that %Co metal decreases from ~60% in fresh samples to ~45% in treated samples (activated RO1 and activated RO2).

Table 8.2 Linear combination fittings of promoted 25%Co/Al_2O_3 catalysts (i.e., before and after simulated regeneration cycles and re-activation) with Co^0 and CoO*

Catalyst	Condition	% weight	
		Co^0	CoO
1.0%Pt-25%Co/Al_2O_3	Freshly activated	73.4	26.6
	Activated RO1	77.7	22.3
	Activated RO2	71.7	28.3
0.52%Ru-25%Co/Al_2O_3	Freshly activated	75.5	24.5
	Activated RO1	83.5	16.5
	Activated RO2	79.3	20.7
0.95%Re-25%Co/Al_2O_3	Freshly activated	72.4	27.6
	Activated RO1	75.1	24.9
	Activated RO2	76.4	23.6
0.55%Ag-25%Co/Al_2O_3	Freshly activated	74.7	25.3
	Activated RO1	73.0	27.0
	Activated RO2	75.7	24.3
1.0%Au-25%Co/Al_2O_3	Freshly activated	59.8	40.2
	Activated RO1	44.9	55.1
	Activated RO2	45.1	55.0
0.53%Rh-25%Co/Al_2O_3	Freshly activated	72.0	28.0
	Activated RO1	76.7	23.3
	Activated RO2	74.7	25.3
0.99%Ir-25%Co/Al_2O_3	Freshly activated	87.0	13.0
	Activated RO1	84.6	15.4
	Activated RO2	79.1	21.0

* The CoO reference spectrum was obtained during a TPR trajectory from the point of maximum CoO content of a 0.5%Pt-25%Co/Al_2O_3 catalyst during TPR-XANES (Jacobs et al., 2007). The white line intensity from this catalyst was found to be slightly higher than that of a bulk CoO reference compound, and thus more appropriate as a reference.

This XANES results are in good agreement with the TPR results of Figure 8.2(E), in which the reduction temperature of Au-promoted catalyst shifts to higher temperature after undergoing simulated regeneration cycles. The loss in the

promoting property of Au after simulated regeneration cycles may be because Au is no longer in good contact with Co oxide after treatment cycles, perhaps as a result of Au agglomeration. Figure 8.3(F) illustrates the XANES spectra of the 0.53%Rh-25%Co/Al_2O_3 catalyst. It is obvious that XANES spectrum of the freshly reduced sample appears to be closer to that of Co metal rather than to CoO and, after undergoing treatment cycles and reactivation (i.e., activated RO1 and activated RO2), the catalyst spectra remain almost identical to that of the freshly reduced catalyst. Examining LC fitting results in Table 8.2, it is evident that the catalyst still maintains a high percentage of Co reduction even after OR cycles (and reactivation), and the wt. % of Co is > 70%. This result is consistent with the TPR result of Figure 8.2(F). Therefore, Rh metal not only facilitates Co oxide reduction but also maintains its ability to promote Co oxide reduction even after simulated regeneration cycles. The last promoter examined was Ir, and normalized XANES spectra of 0.99%Ir-25%Co/Al_2O_3 are shown in Figure 8.3(G). Like the other promoters examined in this work, Ir also does an excellent job in facilitating Co oxide reduction. Interestingly, Ir seems to be the most effective promoter, in that the XANES spectra at the Co K-edge more closely resemble that of Co metal even after simulated regeneration cycles (and reactivation). As summarized in Table 8.2, the percentage of Co metal is higher compared to other metal-promoted catalysts. This is also in agreement with a previous report suggesting that Ir is more efficient than Pt and Ru in facilitating Co oxide reduction (Bianchi, 2001). However, Co metal content appears to decrease with the number of simulated regeneration cycles (and reactivation), and especially after 2 cycles, in which the percentage of Co metal dropped by 8% by weight (i.e., more cobalt present in the oxidized state). This correlates well with the TPR profile of the RO2 sample in Figure 8.2(G), in that the reduction temperature of the RO2 sample shifts to higher temperature relative to that of the RO1 sample. Although Ir initially seems to be the best promoter among those examined in this study from the standpoint of initial reduction, when considering the losses in % reduction as a function of number of cycles, it may prove to be problematic for commercial applications. That is, a more complex regeneration procedure may be required.

8.5 Conclusion

In conclusion, Pt and Re, which are currently used as common promoters for Co/Al_2O_3 FT catalysts, show a capability to maintain their ability to facilitate cobalt oxide reduction after oxidation-reduction cycles, and this is important from the perspective of catalyst regeneration. Ru appears to exhibit some promoter-cobalt segregation with number of simulated regeneration cycles. Rh and Ir were further-examined in this work, and while both metals can facilitate initial Co oxide reduction as well as Pt, Ru, and Re promoters, Rh conserves its ability to facilitate Co oxide reduction after treatment cycles, while some separation between Ir and Co appears to be occurring. In previous work Au and Ag were suggested as possible alternative promoters, and exhibited some benefits in terms of selectivity relative to the unpromoted catalyst. Here it is shown that Au is able to facilitate Co oxide reduction but gradually loses this function after simulated regeneration cycles. On the other hand, Ag is able to facilitate Co oxide reduction as well as Pt, Ru, Re, and Rh, and furthermore, it appears to maintain this function even after simulated regeneration cycles, maintaining more than 70% by weight Co metal even after 2 oxidation-reduction cycles (and reactivation). Ag thus far offers a number of distinct advantages: (1) cost; (2) ability to facilitate reduction of cobalt oxides and maintain this function after oxidation-reduction cycles; and (3) improvements in product selectivity. The next step will be to determine whether the activity of the Ag-promoted Co/alumina catalyst can be regenerated, and to determine if any surface enrichment by Ag occurs with simulated regeneration cycles that may be detrimental to catalyst performance.

8.6 Acknowledgements

This work was supported in part by a grant from the state of Wyoming Clean Coal Research Program for a project entitled "Fischer-Tropsch conversion of Wyoming coal-derived syngas using a small channel reactor for improving efficiency and limiting emissions." We further acknowledge the support of the Commonwealth of Kentucky. We are also grateful to the Fulbright-TRF scholarship program for financial support for Mr. Thani Jermwongratanachai.

8.7 References

Arnoldy, P. and Moulijn, J.A. (1985) Temperature-programmed reduction of CoO Al_2O_3 catalysts. Journal of Catalysis, 93(1), 38-54.

Bazin, D., Borkó, L., Koppány, Z., Kovács, I., Stefler, G., Sajó, L.I., Schay, Z., and Guczi, L. (2002) Re-Co/NaY and Re-Co/Al_2O_3 Bimetallic catalysts: In situ EXAFS study and catalytic activity. Catalysis Letters, 84(3-4), 169-182.

Bianchi, C. (2001) TPR and XPS investigations of Co/Al_2O_3 catalysts promoted with Ru, Ir and Pt. Catalysis Letters, 76(3-4), 155-159.

Cook, K.M., Poudyal, S., Miller, J.T., Bartholomew, C.H., and Hecker, W.C. (2012) Reducibility of alumina-supported cobalt Fischer–Tropsch catalysts: Effects of noble metal type, distribution, retention, chemical state, bonding, and influence on cobalt crystallite size. Applied Catalysis A: General, 449, 69-80.

Das, T.K., Jacobs, G., Patterson, P.M., Conner, W.A., Li, J., and Davis, B.H. (2003) Fischer-Tropsch synthesis: Characterization and catalytic properties of rhenium promoted cobalt alumina catalysts. Fuel, 82(7), 805-815.

Espinoza, R.L., Visagie, J.L., Van Berge, P.J., Bolder, F.H. (1998). US Patent 5,733,839.

Guczi, L., Bazin, D., Kovács, I., Borkó, L., Schay, Z., Lynch, J., Parent, P., Lafon, C., Stefler, G., Koppány, Z., and Sajó, I. (2002) Structure of Pt–Co/Al_2O_3 and Pt–Co/NaY bimetallic catalysts: Characterization by in situ EXAFS,

TPR, XPS and by activity in Co (carbon monoxide) hydrogenation. Topics in Catalysis, 20(1-4), 129-139.

Iglesia, E., Soled, S.L., Fiato, R.A., and Via, G.H. (1993) Bimetallic synergy in cobalt ruthenium Fischer-Tropsch synthesis catalysts. Journal of Catalysis, 143(2), 345-368.

Jacobs, G., Chaney, J.A., Patterson, P.M., Das, T.K., and Davis, B.H. (2004) Fischer–Tropsch synthesis: study of the promotion of Re on the reduction property of Co/Al_2O_3 catalysts by in situ EXAFS/XANES of Co K and Re L_{III} edges and XPS. Applied Catalysis A: General, 264(2), 203-212.

Jacobs, G., Chaney, J.A., Patterson, P.M., Das, T.K., Maillot, J.C., and Davis, B.H. (2004) Fischer-Tropsch synthesis: Study of the promotion of Pt on the reduction property of Co/Al_2O_3 catalysts by in situ EXAFS of Co K and Pt L_{III} edges and XPS. Journal of Synchrotron Radiation, 11(5), 414-422.

Jacobs, G., Das, T.K., Zhang, Y., Li, J., Racoillet, G., and Davis, B.H. (2002) Fischer–Tropsch synthesis: support, loading, and promoter effects on the reducibility of cobalt catalysts. Applied Catalysis A: General, 233(1–2), 263-281.

Jacobs, G., Ji, Y., Davis, B.H., Cronauer, D., Kropf, A.J., and Marshall, C.L. (2007) Fischer–Tropsch synthesis: Temperature programmed EXAFS/XANES investigation of the influence of support type, cobalt loading, and noble metal promoter addition to the reduction behavior of cobalt oxide particles. Applied Catalysis A: General, 333(2), 177-191.

Jacobs, G., Ma, W., Gao, P., Todic, B., Bhatelia, T., Bukur, D.B., Khalid, S., and Davis, B.H. (2012) Fischer-tropsch synthesis: Differences observed in local atomic structure and selectivity with Pd compared to typical promoters (Pt, Re, Ru) of Co/Al_2O_3 catalysts. Topics in Catalysis, 55(11-13), 811-817.

Jacobs, G., Patterson, P.M., Das, T.K., Luo, M., and Davis, B.H. (2004) Fischer–Tropsch synthesis: effect of water on Co/Al_2O_3 catalysts and XAFS characterization of reoxidation phenomena. Applied Catalysis A: General, 270(1–2), 65-76.

Jacobs, G., Ribeiro, M.C., Ma, W., Ji, Y., Khalid, S., Sumodjo, P.T.A., and Davis, B.H. (2009) Group 11 (Cu, Ag, Au) promotion of $15\%Co/Al_2O_3$ Fischer–

Tropsch synthesis catalysts. Applied Catalysis A: General, 361(1–2), 137-151.

Jacobs, G., Sarkar, A., Ji, Y., Luo, M., Dozier, A., and Davis, B.H. (2007) Fischer–Tropsch Synthesis: Assessment of the ripening of cobalt clusters and mixing between Co and Ru promoter via oxidation–reduction-cycles over lower Co-loaded Ru–Co/Al_2O_3 catalysts. Industrial & Engineering Chemistry Research, 47(3), 672-680.

Jermwongratanachai, T., Jacobs, G., Ma, W., Shafer, W.D., Gnanamani, M.K., Gao, P., Kitiyanan, B., Davis, B.H., Klettlinger, J.L.S., Yen, C.H., Cronauer, D.C., Kropf, A.J., and Marshall, C.L. (2013) Fischer–Tropsch synthesis: Comparisons between Pt and Ag promoted Co/Al_2O_3 catalysts for reducibility, local atomic structure, catalytic activity, and oxidation–reduction (OR) cycles. Applied Catalysis A: General, 464–465, 165-180.

Jongsomjit, B., Panpranot, J., and Goodwin Jr, J.G. (2001) Co-support compound formation in alumina-supported cobalt catalysts. Journal of Catalysis, 204(1), 98-109.

Kogelbauer, A., Goodwin Jr, J.G., and Oukaci, R. (1996) Ruthenium promotion of Co/Al_2O_3 Fischer-Tropsch catalysts. Journal of Catalysis, 160(1), 125-133.

Leite, L., Stonkus, V., Ilieva, L., Plyasova, L., Tabakova, T., Andreeva, D., and Lukevics, E. (2002) Promoting effect of gold on the structure and activity of Co/kaolin catalyst for the 2,3-dihydrofuran synthesis. Catalysis Communications, 3(8), 341-347.

Ma, W., Jacobs, G., Ji, Y., Bhatelia, T., Bukur, D., Khalid, S., and Davis, B. (2011) Fischer–Tropsch synthesis: Influence of CO conversion on selectivities, H_2/CO usage ratios, and catalyst stability for a Ru promoted Co/Al_2O_3 catalyst ssing a slurry phase reactor. Topics in Catalysis, 54(13-15), 757-767.

Rønning, M., Nicholson, D., and Holmen, A. (2001) In situ EXAFS study of the bimetallic interaction in a rhenium-promoted alumina-supported cobalt Fischer–Tropsch catalyst. Catalysis Letters, 72(3-4), 141-146.

Rygh, L.E.S., and Nielsen, C.J. (2000) Infrared study of CO adsorbed on a Co/Re/γ-Al_2O_3-based Fischer-Tropsch catalyst. Journal of Catalysis, 194(2), 401-409.

Sadeqzadeh, M., Karaca, H., Safonova, O.V., Fongarland, P., Chambrey, S., Roussel, P., Griboval-Constant, A., Lacroix, M., Curulla-Ferré, D., Luck, F., and Khodakov, A.Y. (2011) Identification of the active species in the working alumina-supported cobalt catalyst under various conditions of Fischer–Tropsch synthesis. Catalysis Today, 164(1), 62-67.

Schanke, D., Hilmen, A.M., Bergene, E., Kinnari, K., Rytter, E., Ådnanes, E., and Holmen, A. (1995) Study of the deactivation mechanism of Al_2O_3-supported cobalt Fischer-Tropsch catalysts. Catalysis Letters, 34(3-4), 269-284.

Schanke, D., Vada, S., Blekkan, E.A., Hilmen, A.M., Hoff, A., and Holmen, A. (1995) Study of Pt-promoted cobalt CO hydrogenation catalysts. Journal of Catalysis, 156(1), 85-95.

Van Berge, P.J., Barradas, S., Van De Loodsrecht, J., and Visagie, J.L. (2001) Advances in the cobalt catalyzed Fischer-Tropsch synthesis. Erdoel Erdgas Kohle, 117(3), 138-142.

Van Berge, P.J., van de Loosdrecht, J., Barradas, S., and van der Kraan, A.M. (2000) Oxidation of cobalt based Fischer–Tropsch catalysts as a deactivation mechanism. Catalysis Today, 58(4), 321-334.

Van Steen, E., Claeys, M., Dry, M.E., Van De Loosdrecht, J., Viljoen, E.L., and Visagie, J.L. (2005) Stability of nanocrystals: Thermodynamic analysis of oxidation and re-reduction of cobalt in water/hydrogen mixtures. Journal of Physical Chemistry B, 109(8), 3575-3577.